# A polarization-independent liquid crystal phase modulation using polymer-network liquid crystals in a 90° twisted cell

Yi-Hsin Lin, Ming-Syuan Chen, Wei-Chih Lin, and Yu-Shih Tsou

Citation: Journal of Applied Physics **112**, 024505 (2012); doi: 10.1063/1.4737260
View online: http://dx.doi.org/10.1063/1.4737260
View Table of Contents: http://scitation.aip.org/content/aip/journal/jap/112/2?ver=pdfcov
Published by the AIP Publishing

# A polarization-independent liquid crystal phase modulation using polymer-network liquid crystals in a 90° twisted cell

Yi-Hsin Lin,[a] Ming-Syuan Chen, Wei-Chih Lin, and Yu-Shih Tsou
*Department of Photonics, National Chiao Tung University, Hsinchu, Taiwan 30010, Taiwan*

(Received 9 May 2012; accepted 8 June 2012; published online 18 July 2012)

A polarization-independent liquid crystal phase modulation using polymer-network liquid crystals in a 90° twisted cell (T-PNLC) is demonstrated. T-PNLC consists of three layers. Liquid crystal (LC) directors in the two layers near glass substrates are orthogonal to each other and those two layers modulate two eigen-polarizations of an incident light. As a result, two eigen-polarizations of an incident light experience the same phase shift. In the middle layer, LC directors are perpendicular to the glass substrate and contribute no phase shift. The phase shift of T-PNLC is electrically tunable and polarization-independent. T-PNLC does not require any bias voltage for operation. The phase shift is 0.28 $\pi$ rad for the voltage of 30 $V_{rms}$. By measuring and analyzing the optical phase shift of T-PNLC at the oblique incidence of transverse magnetic wave, the pretilt angle of LC directors and the effective thickness of three layers are obtained and discussed. The potential applications are spatial light modulators, laser beam steering, and micro-lens arrays.
 [http://dx.doi.org/10.1063/1.4737260]

## I. INTRODUCTION

Liquid crystal (LC) phase-only modulations without mechanical moving parts are important in many applications, such as laser beam steering,[1] tunable focus lenses,[2–6] electrically tunable gratings and prisms,[7] and spatial light modulators.[8] However, the optical efficiency is reduced by the polarizers. As a result, developing a polarization independent LC phase modulator is necessary. Four types of polarization independent LC phase modulators have been demonstrated.[9–16,18] One is residual phase type of LC phase modulations.[9–12] The orientations of LC directors are randomly dispersed. As a result, any polarization of incident light experiences the same averaged refractive index which is related to the same phase shift. The second type is a double-layered type of LC phase modulations.[9,13,14] The structure is based on two homogeneous LC layers with orthogonal rubbing directions. Each LC layer modulates one of the eigen-polarizations of an incident light. As a result, two eigen-polarizations of an incident light experience the same phase shift. The third type is mixed type of LC phase modulations which is the combination of the residual phase type and the double-layered type.[15] The fourth type is based on the optical isotropy induced by Kerr effect of BP-LC.[16] In the double-layered type, the structure with two separated LC layers is difficult to fabricate and the response time is slow (~200 ms).[13,14] The LC phase modulator using 90° twisted nematic liquid crystals was proposed in 1988.[17] A 90° twisted dual-frequency liquid crystals (T-DFLC) with an in-cell double-layered structure can improve the response time (~1.7 ms).[18] However, the required bias voltage (>5.5 $V_{rms}$) and the unavoidable heating effect of dual-frequency liquid crystals hinder the practical applications.[19,20] In addition, no experiments and theoretically analysis discuss about the orientation of LC directors and the effective double-layered thickness in T-DFLC in detail. In this paper, a polarization-independent liquid crystal phase modulation using polymer-network liquid crystals in a 90° twisted cell (T-PNLC) is demonstrated. T-PNLC consists of three layers. LC directors in the two layers near glass substrates are orthogonal to each other and those two layers modulate two eigen-polarizations of an incident light. As a result, two eigen-polarizations of an incident light experience the same phase shift. In the middle layer, LC directors are perpendicular to the glass substrate and contribute no phase shift. Thus, the phase shift of T-PNLC is electrically tunable and polarization-independent. T-PNLC does not require any bias voltage for operation. By measuring and analyzing the optical phase shift of T-PNLC at the oblique incidence of transverse magnetic (TM) wave, the orientation of LC directors and the effective double-layered thickness are obtained and discussed in detail. The potential applications are spatial light modulators, laser beam steering, and micro-lens arrays.

## II. STRUCTURE AND OPERATING PRINCIPLES

Figures 1(a)–1(c) depict the structure and operating principles of polarization independent LC phase modulation using T-PNLC. The structure consists of two ITO glass substrates, two alignment layers, LC directors located in the domains surrounding by polymer networks which are perpendicular to the glass substrates. The formed polymer networks are perpendicular to the glass substrates because the homeotropic texture of the polymer appears in the presence of a sufficiently high electric field when the cell is exposed to UV irradiation for photo-polymerization.[21] As a result, the polymers aggregate to form pillars after polymerization. The polymer networks are made of polymer grains. The rubbing directions of two alignment layers are orthogonal to each other (i.e., x- and y-directions). As a result, without applied voltage (V), LC directors near two glass substrates are also orthogonal to each other. The effective thickness of two LC layers near two glass substrates is $d_1$. In the middle of T-PNLC or the bulk region of T-PNLC, the LC directors are

[a]Electronic mail: yilin@mail.nctu.edu.tw.

 

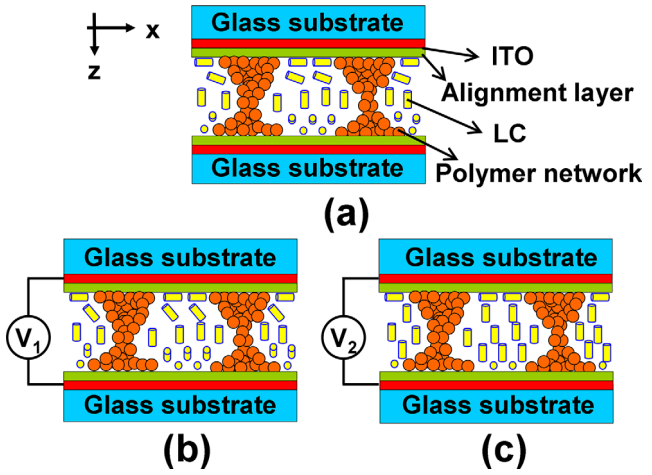


FIG. 1. Structure and operating principles of T-PNLC. (a) At $V=0$, LC directors near two glass substrates are orthogonal to each other, and LC directors are parallel to z-direction in the middle region. (b) At $V_1 > V_{th}$, LC directors near two glass substrates are reoriented by the electric field. (c) At $V_2 \gg V_{th}$, LC directors are perpendicular to the glass substrate.

parallel to z-direction with an effective thickness of $d_2$, as shown in Fig. 1(a). The reason why LC directors parallel to z-direction in the bulk region is because the polymerization process with a high enough curing voltage results in a high tilt angle of LC directors in the bulk region and then the pillar-like polymer networks hold the LC directors in the bulk region after polymerization process. The cell gap (d) then equals to $(2d_1 + d_2)$. At $V=0$, the T-PNLC is operated as a double-layered type phase modulator in which two orthogonal LC layers near glass substrates are separated by the middle LC layers where LC directors parallel to the z direction. When an unpolarized light which can be decomposed into two linear eigen-modes, x and y linearly polarized lights, passes through the T-PNLC along +z direction, each eigen-mode experiences the same phase shift. When the applied voltage is larger than the threshold voltage (i.e., $V_1 > V_{th}$ in Fig. 1(b)), LC directors tend to reorientate along z direction. Two eigen-modes still experience the same phase shift. As a result, the phase shift of T-PNLC is polarization independent. The optical mechanism of the polarization independent double-layered type phase modulation in the similar structure has been reported.[18] At $V=0$, the accumulated phase ($\delta(V=0)$) of T-PNLC for an unpolarized light at a normal incidence can be expressed as

$$\delta(V=0) = k \times [n_1(\theta_p) \times d_1 + n_o \times (d_1 + d_2)], \quad (1)$$

where k is the wave number of incident light, $n_o$ is the ordinary refractive index of LC materials, $n_1$ is the effective refractive index of LC materials, and $\theta_p$ is the pretilt angle of LC directors. When we apply a large voltage (i.e., $V_2 \gg V_{th}$ in Fig. 1(c)), the LC directors are perpendicular to the glass substrates except the LC directors very closed to two alignment layers, as shown in Fig. 1(c). The accumulated phase ($\delta(V_2)$) for an unpolarized incident light at a normal incidence can be expressed as

$$\delta(V_2 \gg V_{th}) = k \times n_o \times (2 \times d_1 + d_2). \quad (2)$$

The difference of the phase shift ($\Delta\delta$) between high voltage ($V_2$) and 0 (i.e., $\Delta\delta \equiv \delta(V=0) - \delta(V_2 \gg V_{th})$) is

$$\Delta\delta = k \times [(n_1(\theta_p) - n_o) \times d_1]. \quad (3)$$

Therefore, we can realize a polarization independent phase modulation by operating an applied voltage to T-PNLC, whose difference of the phase shift depends on the effective thickness of $d_1$ near glass substrates, $n_o$, and the pretilt angle of LC directors. The pretilt angle of LC directors is adjustable by controlling the curing voltage ($V_c$) of T-PNLC.

## III. EXPERIMENTS AND DISCUSSIONS

To prepare the sample of T-PNLC, we mixed a positive nematic LC (E7, Merck, $\Delta n = 0.2255$ for $\lambda = 589.3$ nm at 20 °C) with a UV-curable monomer $M_1$(bisphenol-A-dimethacrylate) and photo-initiator (IRG-184, Merck) at 94:5:1 wt. % ratios. The mixture was filled into an empty LC cell at 40 °C. The empty LC cell consisted of two ITO glass substrates which were coated with mechanically buffered polyimide layers as alignment layers for LC molecules. The rubbing directions of two alignment layers were orthogonal. The cell gap was 5.6 $\mu$m. The LC cell at 25 °C was then applied an alternating current (AC) voltage (or a curing voltage, $V_c$) at $f = 1$ kHz and then exposed UV light ($\lambda = 365$ nm) with irradiance of 1.27 mW/cm$^2$ for 40 min. After photo-polymerization, T-PNLC sample was ready for testing.

To observe the morphologies of polymer networks, Figs. 2(a) and 2(b) show scanning electron microscope (SEM) images of the sample with different magnifications after we removed the LC from polymer networks by hexane. The curing voltage ($V_c$) was 4 $V_{rms}$. In Figs. 2(a) and 2(b), the polymer networks consisting of many polymer grains are perpendicular to the glass substrates. The average size of polymer grains is around 0.2 $\mu$m. The domain size of polymer networks is around 10 $\mu$m. To further understand the orientation of LC directors of the sample after photo-polymerization, we observed the sample under two crossed polarizers. Fig. 2(c) shows the image of the sample with a curing voltage of 4 $V_{rms}$. In Fig. 2(c), the sample is dark (square region) under crossed polarizers. When we rotated the sample under crossed polarizers, the sample remained dark. This means the LC directors in the sample are almost perpendicular to the glass substrates, and the sample has low light scattering. The domain size of polymer networks is larger than the wavelength of the visible light and the size of polymer grains is smaller than the wavelength of the visible light; therefore, the light scattering of T-PNLC is low.

To measure the electro-optical properties of the T-PNLC samples, we measured the transmittance of the T-PNLC samples under an applied voltage. The light source was unpolarized He-Ne laser (MELLES GRIOT: 05-LGR-173, $\lambda = 543.5$ nm). A large area photodiode detector (New Focus, Model 2031) was placed at ~30 cm behind the T-PNLC samples which corresponds to ~2° collection angle. A computer controlled LabVIEW data acquisition system was used to apply the voltage to the sample and record the transmittance at the same time. Fig. 3 shows the measured

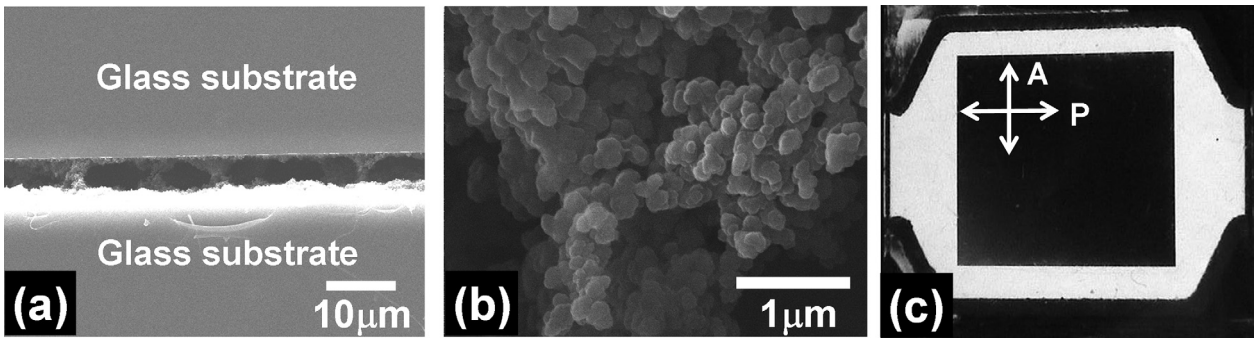


FIG. 2. (a) The side view of SEM image of T-PNLC, and (b) the magnification image of polymer networks of (a). (c) The image of T-PNLC under two crossed polarizers. P and A are the transmissive axes of the polarizer and the analyzer.

transmittance as a function of an applied voltage. For calibrating and comparing the transmittance, we also measured the transmittance of the pure LC sample without any monomer and photoinitiator (gray line in Fig. 3). In Fig. 3, when the curing voltage of T-PNLC is larger than 2.5 $V_{rms}$, the transmittances of T-PNLC samples are closed to the average transmittance of the pure LC sample. Besides, the transmittances of T-PNLC samples remain similar with an increase of an applied voltage. This means the T-PNLC samples are almost transparent when $V_c > 2.5$ $V_{rms}$ which is a requirement for a pure phase modulation. According to measurement, the scattering of T-PNLCs is less than 5%. In order to eliminate the scattering of T-PNLCs, we can adjust the domain size to remove refractive index mismatch between the LC and polymer networks.[22,23]

To measure the phase shifts of T-PNLC samples, we adopted a Mach-Zehnder interferometer. An unpolarized He-Ne laser (JDSU, Model 1122, $\lambda = 633$ nm) was split equally into two arms by a beam splitter, and then two beams recombined again by the other beam splitter. The interference fringes can be observed when two beams are overlapped. Our sample was put in one arm of the interferometer. The fringes are recorded by a digital camera (SONY, DCR-HC40). By recording the shifted fringes between the applied voltage and null voltage ($V = 0$), we can obtain the phase shift of the samples. Fig. 3 shows the phase shift of T-PNLC samples as a function of an applied voltage. The phase shift of T-PNLC for $V_c = 2.5$ $V_{rms}$ is around 0.28 $\pi$ (or 0.88) rad and the phase shift of T-PNLC for $V_c = 4$ $V_{rms}$ is around 0.16 $\pi$ (or 0.50) rad. The phase shift decreases when the curing voltage of T-PNLC increases because the pretilt angle of LC directors of T-PNLC at $V = 0$ is high as the curing voltage is high and then LC directors are almost perpendicular to the glass substrate. According to the experiments, the T-PNLCs have no threshold voltage because of a high pretilt angle of T-PNLCs. The behavior of no threshold voltage in a hybrid aligned nematic cell has been reported.[24,25] In order to exam the polarization dependency, we measured the phase shift as we put a polarizer in front of the unpolarized laser and rotated the polarizer. The phase shift remained the same under different angles of the polarizer, as shown in Fig. 3. This means T-PNLC samples have pure phase modulations and the phase of T-PNLC is polarization independent as well. The phase shifts of T-PNLC samples (0.16 $\pi$-0.28 $\pi$ rad) are larger than both of the residual phase type ($<0.05$ $\pi$ rad) and mixed type of SP-PDLC ($\sim 0.09$ $\pi$ rad).[10–12,15] The total response time, rise time plus decay time, is around 1.6 ms when the T-PNLC is applied a square burst at $f = 1$ kHz between 0 and 30 $V_{rms}$. The fast response is because the polymer networks assist liquid crystal directors relax back.

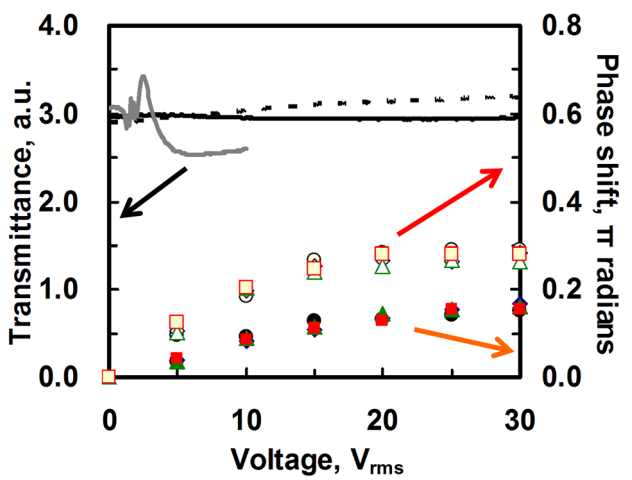


FIG. 3. Transmittance as a function of voltage for pure LC cell (gray line), T-PNLC at $V_c = 2.5$ $V_{rms}$ (dotted line), and T-PNLC at $V_c = 4$ $V_{rms}$ (black line). Phase shift as a function of voltage for T-PNLC at $V_c = 2.5$ $V_{rms}$ (hollow ones) and T-PNLC at $V_c = 4$ $V_{rms}$ (solid ones). Blue solid/hollow diamonds, green solid/hollow triangles, red solid/hollow squares stand for the angle of polarizer of 0°, 45°, 90°, respectively. Black solid/hollow circles represent unpolarized light.

To further analyze the average pretilt angle of LC directors and the effective thicknesses of LC layers (i.e., $d_1$ and $d_2$ in Fig. 4), we measured the phase shift when the incident light ($\lambda = 632.8$ nm) is at the different oblique angles ($\psi$). The relative coordinate between the incident light and the sample is illustrated in Fig. 4. The incident light is TM wave which means the polarization is parallel to the plane of incidence. In the T-PNLC sample, the LC layer can be divided by three effective layers with thicknesses of $d_1$, $d_2$, and $d_1$. The thicknesses of layers 1 and 3 are the same is because LC directors in two layers are affected by the same surface anchoring energy from alignment and polymer networks. When the light is incident into the T-PNLC (at $V = 0$) at $+\psi$ with respect to the normal direction of the T-PNLC, the total accumulated phase of T-PNLC contributed by three layers can be expressed as

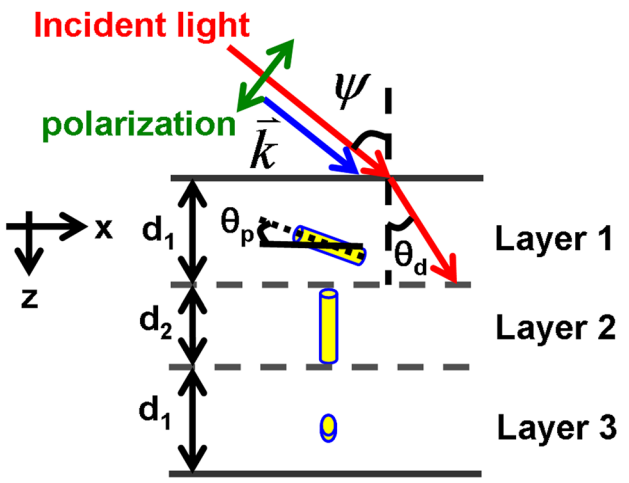


FIG. 4. The illustration of the relative coordinates between the incident-oblique light and the sample.

$$\delta_\psi(V=0) = \delta_1(\theta_p, d_1, \psi) + \delta_2(d_2, \psi) + \delta_3(\theta_p, d_1, \psi), \quad (4)$$

where $\theta_p$ is the pretilt angle, and $\delta_1$, $\delta_2$, and $\delta_3$ are the phases contributed from layers 1, 2, and 3, respectively. Defined that k is the wave number, $n_1$ is an effective refractive index in layer 1, and $d_1'$ is the length when the light passes through layer 1. $\delta_1$ is then equal to $[k \times n_1(\theta_p, \psi) \times d_1'(\theta_p, d_1, \psi)]$. $n_1$ can also be expressed as

$$n_1 = 1 \Big/ \sqrt{\sin^2(\theta_p + \theta_d)/n_o^2 + \cos^2(\theta_p + \theta_d)/n_e^2}, \quad (5)$$

where $\theta_d$ is the refraction angle, $n_o$ is the ordinary refractive index of LC (~1.5189), and $n_e$ is the extraordinary refractive index of LC (~1.7305). $\theta_d$ can be written as[26]

$$\theta_d = \tan^{-1}\frac{k_x}{k_{tz}}, \quad (6)$$

where $k_x$ is the x-component of wave vector in the air and $k_{tz}$ is the z-component of transmitted wave vector in layer 1. $k_x$ and $k_{tz}$ can be further expressed as

$$k_x = (2 \times \pi/\lambda) \times \sin\psi, \quad (7)$$

$$k_{tz} = \frac{n_o}{n_e} \times \left[(B \times k_x + \sqrt{k_o^2 \times n_e^2 \times A - k_x^2})/A\right], \quad (8)$$

where A and B satisfy the following relations:

$$A = \cos^2(90^\circ - \theta_p) + \frac{n_e^2}{n_o^2} \times \sin^2(90^\circ - \theta_p), \quad (9)$$

$$B = \frac{n_o^2 - n_e^2}{n_o \times n_e} \times \sin(90^\circ - \theta_p) \times \cos(90^\circ - \theta_p). \quad (10)$$

The detail derivative for Eqs. (7)–(10) is listed in the Appendix. In Fig. 4, the long axes of LC directors in layers 2 and 3 are parallel to y-z plane. As a result, the phases contributed by layers 2 and 3 (i.e., $\delta_2 + \delta_3$) for $+\psi$ incidence and $-\psi$ incidence are similar. We define the phase difference ($\Delta\delta'$) is the phase between $+\psi$ incidence and $-\psi$ incidence (i.e., $\Delta\delta'(V=0) \equiv \delta_\psi(V=0) - \delta_{-\psi}(V=0)$). Therefore, $\Delta\delta'$ at V = 0 can be written as

$$\Delta\delta'(V=0) = k \times n_1(\theta_p, \psi) \times d_1'(\theta_p, d_1, \psi) - k \times n_1(\theta_p, -\psi) \times d_1'(\theta_p, d_1, -\psi). \quad (11)$$

When we apply a high voltage ($V \gg V_{th}$), the phase shift ($\Delta\delta_{+\psi}$) between V and null voltage at $+\psi$ incidence is $\Delta\delta_{+\psi} = \delta_{+\psi}(V=0) - \delta_{+\psi}(V \gg V_{th})$. Similarly, the phase shift ($\Delta\delta_{-\psi}$) between V and null voltage at $-\psi$ incidence is $\Delta\delta_{-\psi} = \delta_{-\psi}(V=0) - \delta_{-\psi}(V \gg V_{th})$. $\delta_{+\psi}(V \gg V_{th})$ is closed to $\delta_{-\psi}(V \gg V_{th})$ when $V \gg V_{th}$ because liquid crystal directors tilt up parallel to z-direction. Therefore, $(\Delta\delta_{+\psi} - \Delta\delta_{-\psi})$ equals $(\delta_{+\psi}(V=0) - \delta_{-\psi}(V=0))$ which can be expressed as

$$\Delta\delta_{+\psi} - \Delta\delta_{-\psi} = k \times n_1(\theta_p, \psi) \times d_1'(\theta_p, d_1, \psi) - k \times n_1(\theta_p, -\psi) \times d_1'(\theta_p, d_1, -\psi). \quad (12)$$

According to Eqs. (3) and (12), we can measure the phase shifts of $\Delta\delta_{+\psi}$ and $\Delta\delta_{-\psi}$ at different $\psi$ and then we can calculate $\theta_p$ and $d_1$. $d_1$ as a function of pretilt angle ($\theta_p$) at different $\psi$ is shown in Fig. 5(a) for $V_c = 2.5\ V_{rms}$ and Fig. 5(b)

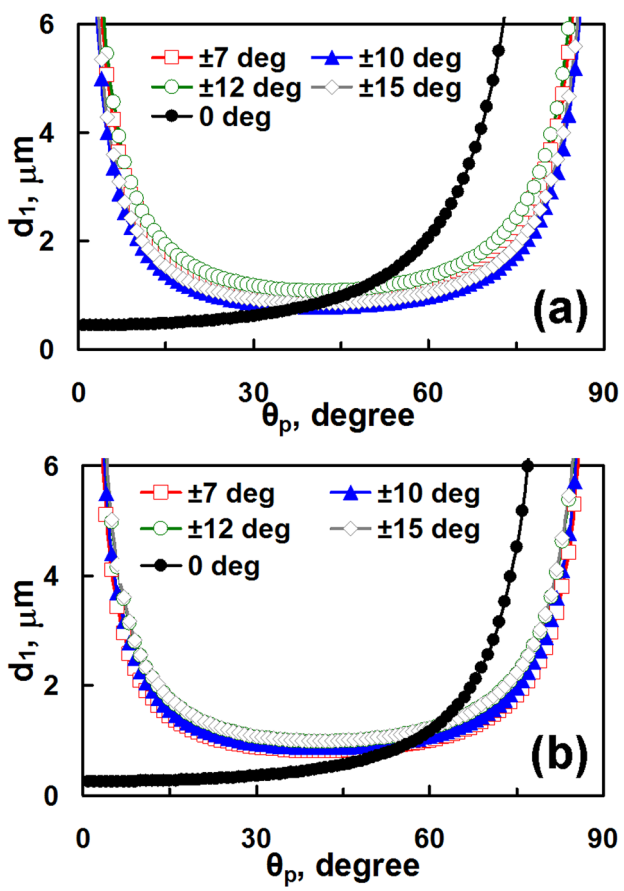


FIG. 5. $d_1$ as a function of $\theta_p$ at different $\psi$ (a) for $V_c = 2.5\ V_{rms}$ and (b) for $V_c = 4\ V_{rms}$. The intersections of the curves represent the solutions of $\theta_p$ and $d_1$. Black solid dots represent $\psi = 0$, red hollow squares represent $\psi = \pm 7^\circ$, blue solid triangles represent $\psi = \pm 10^\circ$, green hollow dots represent $\psi = \pm 12^\circ$, and gray hollow diamonds represent $\psi = \pm 15^\circ$.

for $V_c = 4\ V_{rms}$. In Figs. 5(a) and 5(b), the intersections of the curves represent the solutions of $\theta_p$ and $d_1$. In Fig. 5(a), the pretilt angle is around $43.70° \pm 4.60°$ and $d_1$ is around $0.96 \pm 0.16\ \mu m$ for $V_c = 2.5\ V_{rms}$. In Fig. 5(b), the pretilt angle is around $58.65° \pm 2.75°$ and $d_1$ is around $1.11 \pm 0.18\ \mu m$ for $V_c = 4\ V_{rms}$. The curing voltage is higher; the pretilt angle is larger because the polymer networks provide higher anchoring force to hold the LC directors during curing process at a high voltage. However, $d_1$ is similar ($\sim 1\ \mu m$) when the curing voltage changes. This may because the polymer networks are perpendicular to the glass substrate (Fig. 3) and then the orientation of LC directors near the glass substrates is mainly affected by the anchoring force from two alignment layers. $d_2$ is then calculated around $3.6\ \mu m$ for $d_1$ of $1\ \mu m$. A high curing voltage results in a high pretilt angle, but a high curing voltage can also reduce the polarization independent phase shift.

## IV. CONCLUSION

A polarization-independent liquid crystal phase modulation using T-PNLC is demonstrated. The mechanism of such a phase modulation belongs to double-layered type. The high curing voltage preserved the three sub-layers structures in T-PNLC. The LC directors with high pretilt angle in the layers near glass substrates are orthogonal to each other and the LC directors in the bulk layer are perpendicular to the glass substrate. By measuring and analyzing the optical phase shift of T-PNLC at the oblique incidence of transverse magnetic wave, the pretilt angle of LC directors is $43.70° \sim 58.65°$ depending on the curing voltage and the effective double-layered thickness is $\sim 1\ \mu m$ independent of the curing voltage. The T-PNLC is a pure phase modulation at low operating voltage ($<30\ V_{rms}$) and has fast response time ($\sim 1.6$ ms). The phase shift is $\sim 0.28\ \pi$ rad which is large enough for making micro-lens arrays.[15] To further enlarge the phase shift, we can enlarge the cell gap and increase the birefringence of the LC. The potential applications are spatial light modulators, laser beam steering, and micro-lens arrays.

## ACKNOWLEDGMENTS

This research was supported by the National Science Council (NSC) in Taiwan under the Contract No. 98-2112-M-009-017-MY3.

## APPENDIX: DERIVATIVE OF THE OBLIQUE INCIDENCE

For layer 1 in Fig. 4, the long axis of LC directors is parallel to the plane of incidence and the incident light is TM wave. The refractive index of air is 1. The refraction angle $\theta_d$ can be expressed as

$$\theta_d = \tan^{-1}\frac{k_x}{k_{tz}}, \tag{A1}$$

where $k_x$ is the x-component of the wave vector in the air and $k_{tz}$ is the z-component of transmitted wave vector in layer 1. The x-component of the wave vector in the interface should be continuous. Therefore, $k_x$ can be written as

$$k_x = \frac{2\pi}{\lambda} \times \sin\psi, \tag{A2}$$

where $\psi$ is the incident angle. Consider a coordinate (a,b,c) of a LC director in layer 1, c-axis is parallel to the long axis of LC directors, a-axis perpendicular to the long axis of the LC director is on the x-z plane and b-axis is then parallel to y-axis. By the dispersion relation

$$\frac{k_a^2 + k_b^2}{n_e^2} + \frac{k_c^2}{n_o^2} - k^2 = 0, \tag{A3}$$

where k is the wave vector of incident light and k also equals $2\pi/\lambda$. $\lambda$ is wavelength of the incident light. $k_a$, $k_b$, and $k_c$ are the a-, b-, and c- components of the wave vector in layer 1. $k_b$ should be zero when the plane of incidence is x-z plane. Eq. (A3) can be written as

$$\frac{k_a^2}{n_e^2} + \frac{k_c^2}{n_o^2} - k_o^2 = 0. \tag{A4}$$

We can use the rotation matrix to get the relation between $k_a$, $k_c$ and $k_x$, $k_{tz}$

$$\begin{bmatrix} k_c \\ k_a \end{bmatrix} = \begin{bmatrix} \cos(90° - \theta_p) & \sin(90° - \theta_p) \\ -\sin(90° - \theta_p) & \cos(90° - \theta_p) \end{bmatrix} \begin{bmatrix} k_{tz} \\ k_x \end{bmatrix}, \tag{A5}$$

$$k_a = k_x \times \cos(90° - \theta_p) - k_{tz} \times \sin(90° - \theta_p), \tag{A6}$$

$$k_c = k_x \times \sin(90° - \theta_p) + k_{tz} \times \cos(90° - \theta_p), \tag{A7}$$

where $\theta_p$ is the pretilt angle of LC directors. We can substitute Eqs. (A6) and (A7) to Eqs. (A4) can be expressed as

$$\frac{(k_x \times \cos(90° - \theta_p) - k_{tz} \times \sin(90° - \theta_p))^2}{n_e^2} + \frac{(k_x \times \sin(90° - \theta_p) + k_{tz} \times \cos(90° - \theta_p))^2}{n_o^2} = k_o^2. \tag{A8}$$

By rearranging Eq. (A8) as a polynomial of $k_{tz}$, Eq. (A9) is obtained

$$\frac{A}{n_o^2} \times k_{tz}^2 - \frac{2 \times B}{n_o \times n_e} \times k_x \times k_{tz} + \left(\frac{C}{n_e^2} \times k_x^2 - k_o^2\right) = 0, \tag{A9}$$

where A, B, and C satisfy the following relations:

$$A = \cos^2(90° - \theta_p) + \frac{n_o^2}{n_e^2} \times \sin^2(90° - \theta_p), \tag{A10}$$

$$B = \frac{n_o^2 - n_e^2}{n_o \cdot n_e} \times \sin(90° - \theta_p) \times \cos(90° - \theta_p), \tag{A11}$$

$$C = \cos^2(90° - \theta_p) + \frac{n_e^2}{n_o^2} \times \sin^2(90° - \theta_p), \tag{A12}$$

$$A \times C - B^2 = 1. \tag{A13}$$

By solving Eq. (A9), we can obtain the value of $k_{tz}$

$$k_{tz} = \frac{n_o}{n_e} \times \frac{[B \times k_x + \sqrt{k_o^2 \times n_e^2 \times A - k_x^2}]}{A}. \quad \text{(A14)}$$


[1]P. F. McManamon, T. A. Dorschner, D. L. Corkum, L. J. Friedman, D. S. Hobbs, M. Holz, S. Liberman, H. Q. Nguyen, D. P. Resler, R. C. Sharp, and E. A. Watson, Proc. IEEE **84**, 268 (1996).
[2]H. C. Lin and Y. H. Lin, Appl. Phys. Lett. **97**, 063505 (2010).
[3]Y. H. Lin, M. S. Chen, and H. C. Lin, Opt. Express **19**, 4714 (2011).
[4]H. C. Lin and Y. H. Lin, Appl. Phys. Lett. **98**, 083503 (2011).
[5]H. C. Lin, M. S. Chen, and Y. H. Lin, Trans. Electr. Electron. Mater. **12**, 234 (2011).
[6]H. C. Lin and Y. H. Lin, Opt. Express **20**, 2045 (2012).
[7]H. Ren, Y. H. Fan, and S. T. Wu, Appl. Phys. Lett. **82**, 3168 (2003).
[8]U. Efron, *Spatial Light Modulators* (Marcel Dekker, New York, 1994).
[9]Y. H. Lin, H. Ren, and S. T. Wu, Liq. Cryst. Today **17**, 2 (2009).
[10]Y. H. Lin, H. Ren, Y. H. Fan, Y. H. Wu, and S. T. Wu, J. Appl. Phys. **98**, 43112 (2005).
[11]H. Ren, Y. H. Lin, C. H. Wen, and S. T. Wu, Appl. Phys. Lett. **87**, 191106 (2005).
[12]H. Ren, Y. H. Lin, Y. H. Fan, and S. T. Wu, Appl. Phys. Lett. **86**, 141110 (2005).
[13]Y. H. Lin, H. Ren, Y. H. Wu, Y. Zhao, J. Y. Fang, Z. Ge, and S. T. Wu, Opt. Express **13**, 8746 (2005).
[14]H. Ren, Y. H. Lin, and S. T. Wu, Appl. Phys. Lett. **88**, 61123 (2006).
[15]Y. H. Lin and Y. S. Tsou, J. Appl. Phys. **110**, 114516 (2011).
[16]Y. H. Lin, H. S. Chen, H. C. Lin, Y. S. Tsou, H. K. Hsu, and W. Y. Li, Appl. Phys. Lett. **96**, 113505 (2010).
[17]N. Konforti, E. Marom, and S. T. Wu, Opt. Lett. **13**, 251 (1988).
[18]Y. Huang, C. H. Wen, and S. T. Wu, Appl. Phys. Lett. **89**, 021103 (2006).
[19]C. H. Wen and S. T. Wu, Appl. Phys. Lett. **86**, 231104 (2005).
[20]Y. Yin, S. V. Shiyanovskii, and O. D. Lavrentovich, J. Appl. Phys. **100**, 024906 (2006).
[21]S. T. Wu and D. K. Yang, *Reflective Liquid Crystal Display* (John Wiley & Sons, Inc., New York, 2002).
[22]Y. H. Fan, Y. H. Lin, H. Ren, S. Gauaz, and S. T. Wu, Appl. Phys. Lett. **84**, 1233 (2004).
[23]J. Sun, H. Xianyu, Y. Chen, and S. T. Wu, Appl. Phys. Lett. **99**, 021106 (2011).
[24]S. Matsumoto, M. Kawamoto, and K. Mizunoya, J. Appl. Phys. **47**, 3842 (1976).
[25]Y. Q. Lu, X. Liang, Y. H. Wu, F. Du, and S. T. Wu, Appl. Phys. Lett. **85**, 3354 (2004).
[26]C. A. Bennett, *Principle of Physical Optics* (John Wiley & Sons, Inc., New York, 2008).